NASA Technical Memorandum 81307

NASA-TM-81307 19810020554

(NASA-TM-81307) A VALIDATION OF LTRAN2 WITH HIGH FREQUENCY EXTENSIONS BY COMPARISONS WITH EXPERIMENTAL MEASUREMENTS OF UNSTEADY TRANSONIC FLOWS (NASA) 24 p HC A02/MF A01 CSCL 01A G3/02

N81-29092

Unclas 27100

A Validation of LTRAN2 With High Frequency Extensions by Comparisons With Experimental Measurements of Unsteady Transonic Flows

Kristin A. Hessenius and Peter M. Goorjian

July 1981

National Aeronautics and

NASA Technical Memorandum 81307

A Validation of LTRAN2 With High Frequency Extensions by Comparisons With Experimental Measurements of Unsteady Transonic Flows

Kristin A. Hessenius
Peter M. Goorjian, Ames Research Center, Moffett Field, California

National Aeronautics and Space Administration

Ames Research Center

A VALIDATION OF LTRAN2 WITH HIGH FREQUENCY EXTENSIONS BY COMPARISONS WITH EXPERIMENTAL MEASUREMENTS OF UNSTEADY TRANSONIC FLOWS

Kristin A. Hessenius and Peter M. Goorjian
Ames Research Center

SUMMARY

A high frequency extension of the NASA-Ames unsteady, transonic code LTRAN2 has been created and is evaluated by comparisons with experimental results. The experimental test case is a NACA 64A010 airfoil in pitching motion at a Mach number of 0.8 over a range of reduced frequencies. Comparisons indicate that the modified code is an improvement of the original LTRAN2 and provides closer agreement with experimental lift and moment coefficients. A discussion of the code modifications, which involve the addition of high frequency terms to the boundary conditions of the numerical algorithm, is also included.

I. INTRODUCTION

Computation of unsteady transonic flow about oscillating airfoils is possible through the use of LTRAN2, a computer code developed at NASA-Ames Research Center by Ballhaus and Goorjian in 1976 (ref. 1). LTRAN2 solves the two-dimensional, nonlinear, small-disturbance equation under the low reduced frequency assumption ($k \equiv \omega\, c/U_\infty < 0.2$, where k is the reduced frequency based on full chord, c). For the purpose of flutter analysis, however, industrial users have indicated the need to perform accurate calculations in a frequency range up to k = 1.0. With this in mind, an objective of the present study is to extend the range of reduced frequency for improved LTRAN2 applicability. The modifications made to the code in this study involve the addition of high frequency-time dependent terms in the calculation of the pressure coefficient as well as the wake and downstream boundary conditions. The low frequency governing equation is retained.

Several other researchers (refs. 2-4) have performed similar modifications to LTRAN2, adding high frequency terms to the boundary conditions of the numerical algorithm. Their results indicate that under subsonic flow conditions, improved agreement with linear theory in amplitudes and phase angles of lift and moment coefficients is obtained at higher frequencies with the modified code (ref. 2). However, to truly demonstrate the merit of the modified code, calculations done under transonic conditions should be compared with experimental results. Hence, this study was undertaken to modify the existing code LTRAN2 and to evaluate the effects of these changes by comparison with experimental data.

The test case for comparison (ref. 5) was a NACA 64A010 airfoil, pitching about quarter chord, at a Mach number of 0.8 over a range of reduced frequencies up to 0.6. This case was chosen based on the following criteria:

1) the availability of good test data
2) the presence of a moderate strength shock wave
3) the absence of strong separation effects in the experiments.

The numerical procedure including the code modifications used in the creation of LTRAN2-HI, a high frequency extension of the original code, is discussed in section II. Linear theory comparisons are made in section III which indeed confirm the results of other researchers (refs. 2-4) that, in general, accuracy is improved at higher reduced frequencies. Section III also presents the results of the nonlinear, experimental comparisons where LTRAN2-HI is shown to be superior. Finally, brief concluding remarks are made in section IV.

The authors wish to thank S. S. Davis for supplying the linear theory results, as well as W. J. McCroskey and G. N. Malcolm for their comments and suggestions while reviewing the manuscript.

II. GOVERNING EQUATION AND BOUNDARY CONDITIONS

Governing Equation

An unsteady, transonic small-disturbance equation in Cartesian coordinates may be written as

$$A\phi_{tt} + 2B\phi_{xt} = C\phi_{xx} + \phi_{yy} \tag{1}$$

where

$$A = k^2 M_\infty^2/\delta^{2/3}$$

$$B = k\, M_\infty^2/\delta^{2/3}$$

$$C = (1 - M_\infty^2)/\delta^{2/3} - (\gamma+1)M_\infty^m \phi_x$$

and where ϕ is the disturbance velocity potential, M_∞ is the freestream Mach number, γ is the ratio of specific heats, and δ is the airfoil thickness-to-chord ratio (ref. 6). The choice of the exponent m is somewhat arbitrary. In the calculations presented here, Spreiter scaling was used (m = 2). The parameter k is the reduced frequency. For an airfoil of chord length c, traveling with speed U_∞, and executing some unsteady oscillatory motion of frequency ω, $k \equiv \omega c/U_\infty$. Thus the reduced frequency is given in terms of radians of oscillatory motion per chord length of airfoil travel. The quan-

tities x,y,t,ϕ in equation (1) have been scaled by $c, c/\delta^{1/3}, \omega^{-1}, c\delta^{2/3} U_\infty$, respectively. The right-hand side of equation (1) is the familiar two-dimensional, transonic, small-disturbance equation for steady flows.

An approximation to equation (1), valid for low reduced frequencies, is the equation

$$2B\phi_{xt} = C\phi_{xx} + \phi_{yy} \tag{2}$$

where B and C are defined in equation (1). This equation can also be derived from the unsteady Euler equations under the assumptions

$$k \sim \delta^{2/3} \sim 1-M_\infty^2 << 1 \tag{3}$$

Boundary Conditions and Code Modifications

Code modifications in the conversion of LTRAN2 to LTRAN2-HI introduce time dependent terms in the calculation of the pressure coefficient and the wake and downstream boundary conditions. These changes, which are underlined in the following equations, and the numerical boundary conditions are discussed below in greater detail.

Pressure Coefficient: An expression for the unsteady, small-disturbance pressure coefficient may be written

$$C_p = -2\,(\phi_x + \underline{k\phi_t}) \tag{4}$$

Under the low frequency assumption (original LTRAN2) the $k\phi_t$ term was omitted by an order of magnitude argument. LTRAN2-HI now incorporates high frequency effects in the calculation of C_p by employing equation (4). The differencing scheme used in this calculation is of the Crank- Nicolson type (second order accurate at $\phi_j^{n+1/2}$, where j is the grid index in the x direction) and may be expressed:

$$C_p = -2\left\{ \frac{1}{4}\left[\left(\frac{\phi_{j+1} - \phi_j}{\Delta X_{j+1,j}} + \frac{\phi_j - \phi_{j-1}}{\Delta X_{j,j-1}}\right)^n + \left(\frac{\phi_{j+1} - \phi_j}{\Delta X_{j+1,\,j}} + \frac{\phi_j - \phi_{j-1}}{\Delta X_{j,j-1}}\right)^{n+1}\right] + k\left(\frac{\phi_j^{n+1} - \phi_j^{n}}{\Delta t}\right)\right\}$$

Wake Condition: To ensure a continuity of pressure across the vortex sheet

$$\left[C_p \right] = 0$$

which now implies

$$\left[\phi_x + k \underline{\phi_t} \right] = 0 \qquad (5)$$

where [ ] denote a jump across the wake. The addition of the $k\phi_t$ term in this wake condition constituted the most significant coding change to LTRAN2. Formerly, vorticity in the wake was assumed to propagate infinitely fast downstream (for a characteristic analysis, see reference 1). Circulation, a function of time alone, was then assumed to be uniform in the x spatial direction from the airfoil trailing edge to the downstream boundary. With the inclusion of a time dependent term in the pressure coefficient calculation, enforcement of the jump conditions for the wake produces a circulation quantity now a function of both time and space. Consequently, vorticity travels downstream at a finite velocity (in unscaled units, the freestream velocity) as shown by the following brief characteristic analysis.

Since the circulation $\Gamma = \Delta\phi$, the jump condition from equation (5) yields

$$\Gamma_x + k\Gamma_t = 0 \qquad (6)$$

Equation (6) has characteristics

$$t = kx + \text{constant}$$

and Γ remains constant along these lines. Thus, Γ propagates downstream at a velocity

$$\frac{dx}{dt} = \frac{1}{k} \qquad \text{in scaled units}$$

Recognizing that $x = \bar{x}/c$, $t = \omega\bar{t}$, $k = \omega c/U_\infty$ where $\bar{x}$, $\bar{t}$ are unscaled quantities

$$\frac{d\bar{x}}{d\bar{t}} = U_\infty$$

Therefore the introduction of the $k\phi_t$ term in equation (5) provides a more accurate description of vorticity propagation in the wake at the freestream velocity.

The following Crank-Nicolson algorithm, consistent with the differencing of the governing equation, was chosen to implement the wake condition in LTRAN2-HI.

$$\frac{1}{2}\left\{\left(\frac{\Gamma_j^n - \Gamma_{j-1}^n}{\Delta x_{j,j-1}} + \frac{\Gamma_j^{n+1} - \Gamma_{j-1}^{n+1}}{\Delta x_{j,j-1}}\right) + \left(\Gamma_{i-1}^{n+1} - \Gamma_{i-1}^{n} - \Gamma_i^{n+1} - \Gamma_i^{n}\right)\right\} = 0$$

Solving for the value of circulation at the new time level:

$$\Gamma_j^{n+1} = \Gamma_{j-1}^{n} + \left[\frac{\Delta t - k\,\Delta x_{j,j-1}}{\Delta t + k\,\Delta x_{j,j-1}}\right]\left(\Gamma_{j-1}^{n+1} - \Gamma_j^{n}\right) \qquad (7)$$

Downstream Boundary Condition: The downstream boundary condition (formerly $\phi_x = 0$ as x approaches infinity) becomes

$$\phi_x + k\,\phi_t = 0 \qquad x \to \infty \qquad (8)$$

Like the circulation, the disturbance potential at the downstream boundary is now a function of time and space.

This condition differs from the LTRAN2-NLR (ref. 2) downstream boundary condition where zeroth order extrapolation ($\phi_x = 0$) was retained. However, implementation of equation (8) is believed to maintain consistency at the point of intersection of the wake and downstream boundary conditions. Specifically,

$$\phi_{jmax}^{n+1} = \phi_{jmax-1}^{n} + \left[\frac{\Delta t - k\,\Delta x_{jmax,\,jmax-1}}{\Delta t + k\,\Delta x_{jmax,\,jmax-1}}\right]\left(\phi_{jmax-1}^{n+1} - \phi_{jmax}^{n}\right)$$

where jmax is the grid index of the x-location farthest downstream. Hence equation (7) is also satisfied at j=jmax.

Airfoil Tangency Condition: A time dependent term is included in the body boundary condition thus eliminating the low frequency assumption in the airfoil tangency condition. If $y = f(x,t)$ defines the body surface, then

$$\phi_y = f_x(x,t) + k\,f_t(x,t) \qquad (9)$$

ensures flow tangency.

Although undocumented, equation (9) (including this time dependent term) was used in all published "low frequency" LTRAN2 calculations by Ballhaus and Goorjian. Also, in the calculations presented here, equation (9) will be used by both LTRAN2 and LTRAN2-HI.

III. CALCULATED RESULTS

Linear Calculations

Computed results from LTRAN2 and LTRAN2-HI are first compared with exact linear theory results. This test is to establish the capability of the modified code to provide accurate unsteady solutions in the linear domain. The exact linear theory results are solutions to equation (1) with $\gamma = -1$ in the expression for C. The linear code results are solutions to equation (2), also with $\gamma = -1$. Differences in the comparison may be attributed to two sources: 1) numerical error in the algorithm, and 2) deficiencies in the numerical algorithm resulting from the neglect of the term $A\,\phi_{tt}$ in the governing equation.

Consistent with the findings of Houwink and van der Vooren (ref. 2), LTRAN2 with a high frequency extension provides better agreement with linear theory than the original LTRAN2 in amplitudes and phase angles of lift and moment coefficients. Figures 1 and 2 give lift and moment coefficients versus reduced frequency for the case published in reference 2 (flat plate pitching 0.25° about quarter chord, $\alpha_o = 0°$, $M_\infty = 0.7$). Note that the original LTRAN2 provides reasonably accurate results but only for reduced frequencies less than 0.2. With the exception of the real component of the moment coefficient, LTRAN2-HI provides a more accurate prediction of both lifts and moments over the entire range of reduced frequencies tested. Because of the single favorable comparison of the low frequency LTRAN2 with linear theory (fig. 2a, real component of moment), the high frequency extension is not clearly an improvement of the original code. This fact further motivates a comparison with experimental data.

Nonlinear Experimental Comparisons

As stated previously, comparisons with experimental data for a pitching (1° about quarter chord) NACA 64A010 airfoil were made at a transonic Mach number of 0.8 (ref. 5). All unsteady calculations were initialized with a steady solution found by adjusting the steady angle of attack to match the computed lift value with the experimentally determined steady lift. With a given value of C_l (steady) = -0.029 from experiment, computations were performed at $\alpha_o = -0.1194$ thereby matching lifts. Also, pressure coefficient calculations were sensitive to the type of smoothing used in defining the airfoil coordinate input. Consequently, the smoothed NACA 64A010 experimental coordinates given in reference 5 were used in the computation to maintain some degree of consistency in modeling the experiment.

The computed results of figure 3 represent the initial conditions for the unsteady calculations. Experimental steady lower surface pressures are shown in this figure with the calculated pressures at the same value of lift. This information should be used as a baseline comparison.

In the following computed unsteady results, both LTRAN2 and LTRAN2-HI were run with 360 time steps per cycle for $k > 0.1$. To maintain stability of both codes at the lower reduced frequencies, it was necessary to increase

the number of time steps per cycle to 960 and 1920 for k = 0.1 and k = 0.05, respectively. The modifications to LTRAN2 did not adversely affect the stability of the code. In fact, LTRAN2-HI, unlike its counterpart, was capable of producing a stable solution at k = 0.05 with 1440 time steps per cycle indicating that the addition of high frequency terms has a stabilizing effect on the code. Also, high frequency results may be obtained for essentially the same "price" as results from the original LTRAN2.

Figures 4 and 5 display first harmonic comparisons of lift and leading edge moment coefficients versus reduced frequency (reference 5 reports first harmonic data; computed results were Fourier-analyzed to determine first harmonics). Here LTRAN2-HI shows improved agreement with experiment at higher frequencies. Note in particular the successful prediction by LTRAN2-HI of the critical transition in the leading edge moment from a phase lead to a phase lag (fig. 5b). As shown in figures 4a and 5a, the high frequency modification, in general, produces an improvement in the calculation of real and imaginary components of both lift and moment coefficients over the entire reduced frequency range. The greatest improvement is seen in the determination of the imaginary components where LTRAN2-HI, unlike the original code, captures the experimentally observed trends. For this reason, LTRAN2-HI is the recommended version of the code for use in transonic calculations.

First harmonic unsteady lower surface pressure comparisons are made in figures 6 through 12, spanning the reduced frequency range. Real and imaginary components of the pressure coefficient are presented. However, amplitude and phase information is included for k = 0.1 (fig. 7) to display the somewhat misleading behavior of the calculated phase angle after the shock ($x/c>0.6$). In this region the real component of pressure is relatively small, and therefore a slight error in its computation will produce a large change in phase angle ($\phi = \tan^{-1}$ ($^{Im}/_{Re}$)). Hence the comparison of real and imaginary components with their corresponding experimental values is the preferred method of presentation.

The surface pressure comparisons are found to be inconclusive, however. It is difficult to justify the use of LTRAN2-HI over the use of the original code based on this information alone, for there are instances where the two codes seem equally suitable. But as noted previously in figures 4 and 5, LTRAN2-HI provides improvement in lift and moment calculations, especially in the prediction of the imaginary components of these loads. Consequently, the importance of examining integrated pressures must not be underestimated.

IV. CONCLUSIONS

LTRAN2-HI, a high frequency extension of the NASA-Ames unsteady, small-disturbance code LTRAN2, provides more accurate unsteady results as evidenced by experimental comparisons. The modified code is a versatile tool capable of performing reasonably accurate inviscid calculations in both linear and nonlinear flow regimes. Results from the improved code may be obtained at no extra expense to the user. LTRAN2-HI has now become the default option of the NASA-Ames code LTRAN2.

REFERENCES

1. Ballhaus, W.F.; and Goorjian, P.M.: Implicit Finite Difference Computations of Unsteady Transonic Flows about Airfoils, Including the Treatment of Irregular Shock Wave Motions. AIAA J., vol. 15, no. 12, 1977, pp. 1728-1735.

2. Houwink, R.; and van der Vooren, J.: Improved Version of LTRAN2 for Unsteady Transonic Flow Computations. AIAA J., vol. 18, no. 8, 1980, pp. 1008-1010.

3. Couston, M.; and Angelini, J.J.: Numerical Solutions of Nonsteady Two-Dimensional Transonic Flows. J. Fluids Eng., vol. 101, 1979, pp. 341-347.

4. Rizzetta, D.P.; and Yoshihara, H.: Computations of the Pitching Oscillation of a NACA 64A-010 Airfoil in the Small Disturbance Limit. AIAA Paper 80-0128, Jan. 1980.

5. Davis, S.S.; and Malcolm, G.N.: Experimental Unsteady Aerodynamics of Conventional and Supercritical Airfoils. NASA TM 81221, 1980.

6. Landahl, M.: Unsteady Transonic Flow. Pergamon Press, 1961.

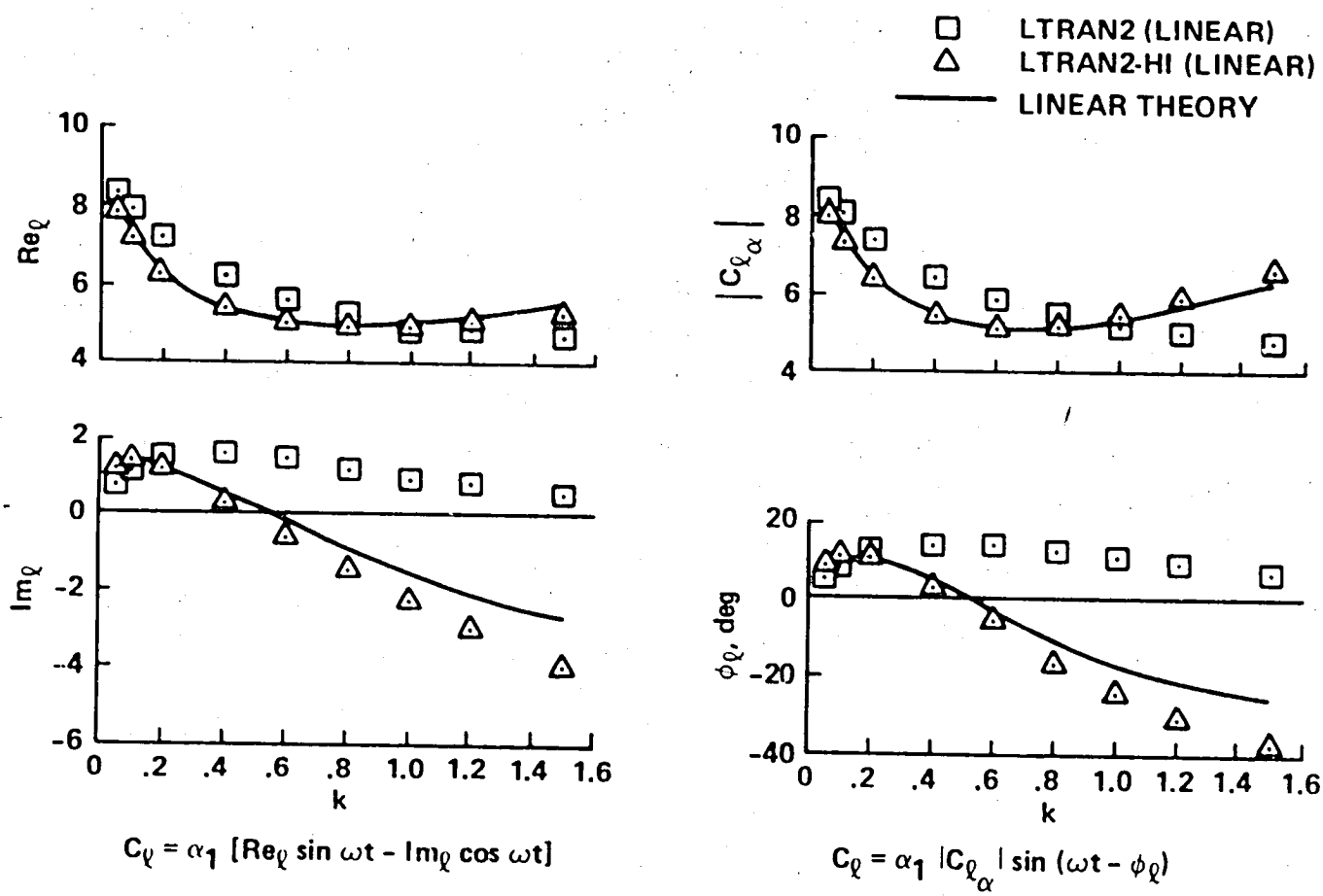

(a) Real and imaginary components.

(b) Amplitude and phase.

Figure 1.- Lift coefficients vs reduced frequency for a pitching flat plate, $M_\infty = 0.7$, $k \equiv \omega c/U_\infty$, $\alpha = \alpha_0 + \alpha_1 \sin \omega t$.

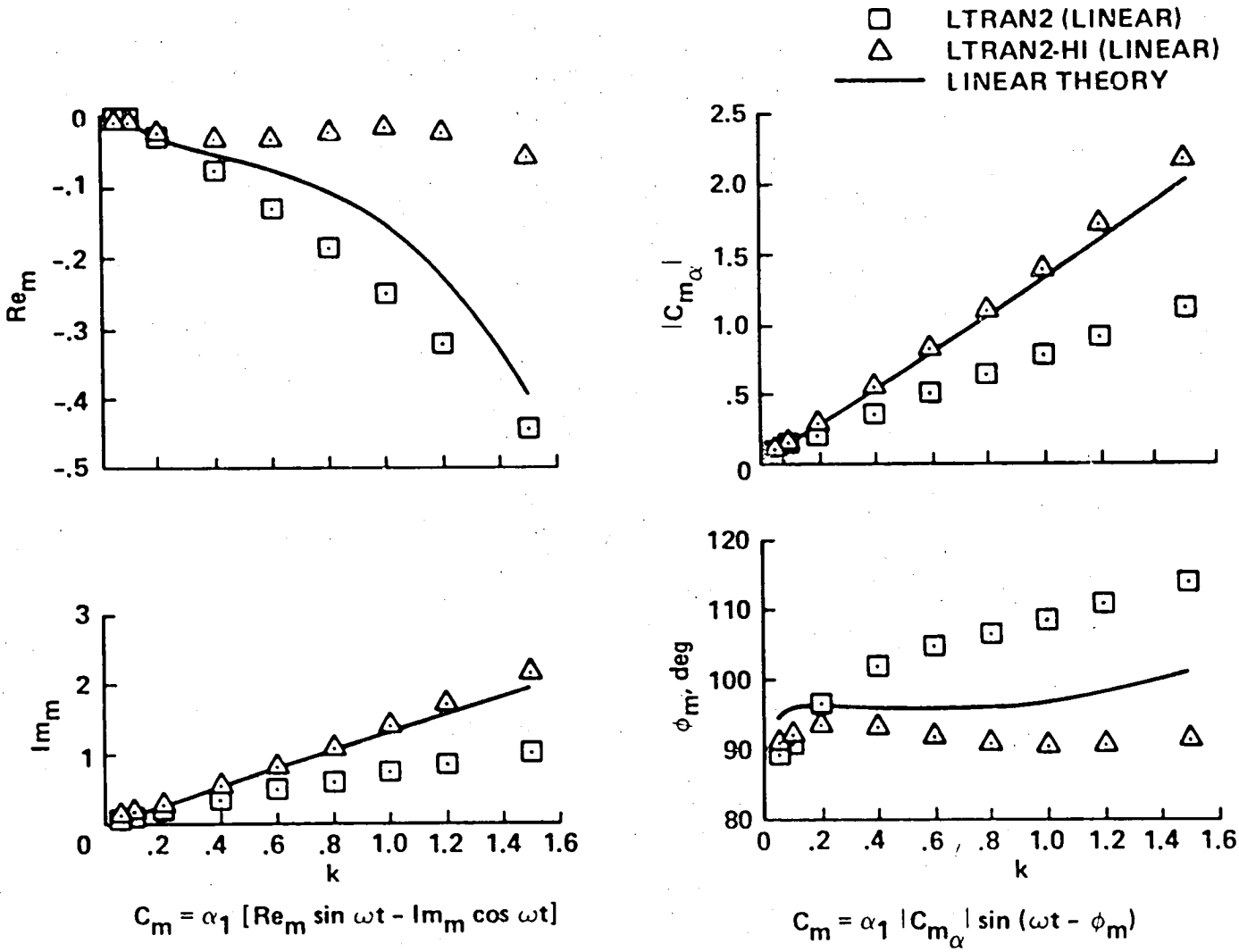

(a) Real and imaginary components.

(b) Amplitude and phase.

Figure 2.- Quarter-chord moment coefficients vs reduced frequency for a pitching flat plate, $M_\infty = 0.7$, $k \equiv \omega c/U_\infty$, $\alpha = \alpha_0 + \alpha_1 \sin \omega t$.

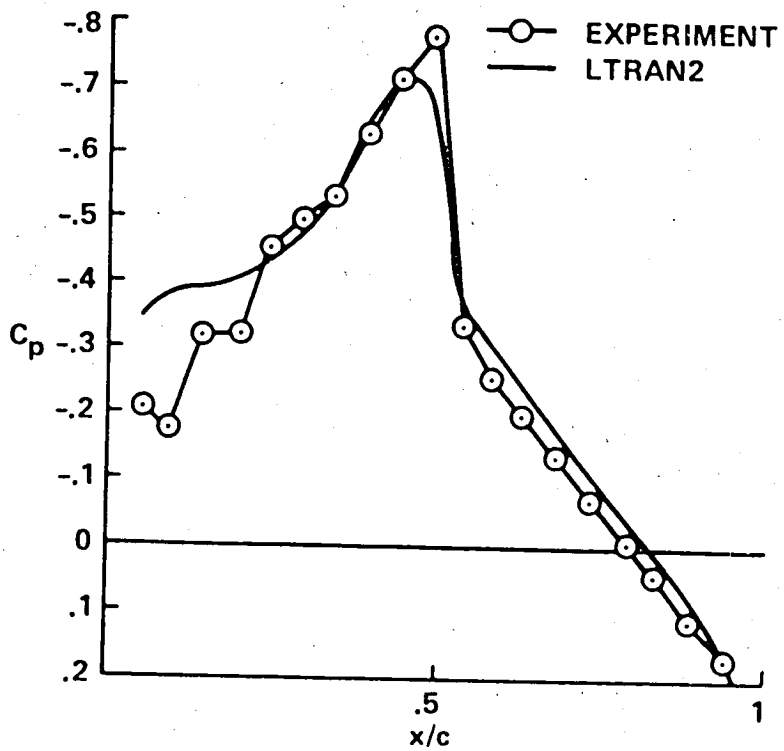

Figure 3.- Steady lower-surface pressure coefficients for a NACA 64A010 airfoil, $M_\infty = 0.8$, $C_\ell = -0.029$.

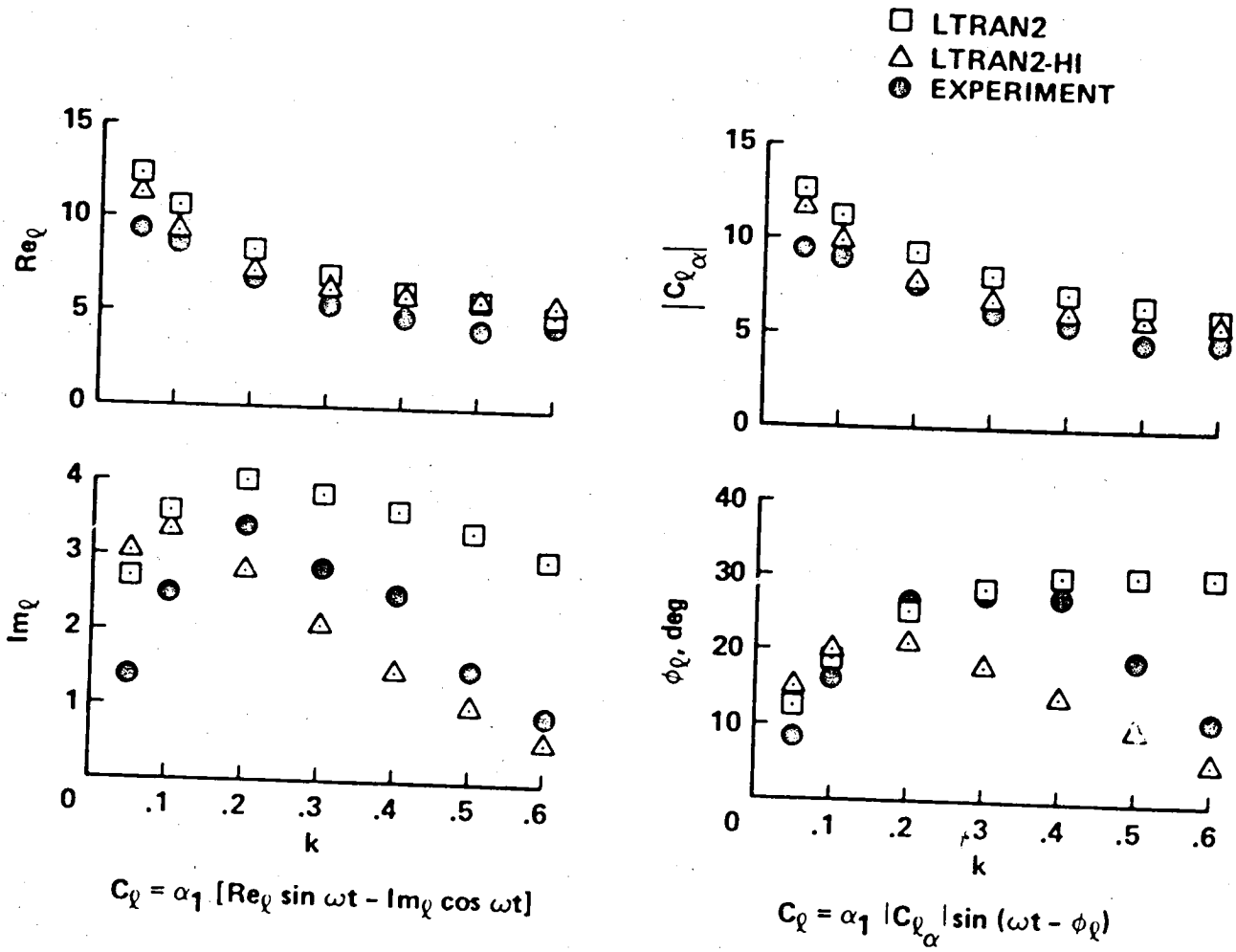

(a) Real and imaginary components.

(b) Amplitude and phase.

Figure 4.- Lift coefficients vs reduced frequency for a pitching NACA 64A010 airfoil, $M_\infty = 0.8$, $k \equiv \omega c/U_\infty$, $\alpha = \alpha_0 + \alpha_1 \sin \omega t$.

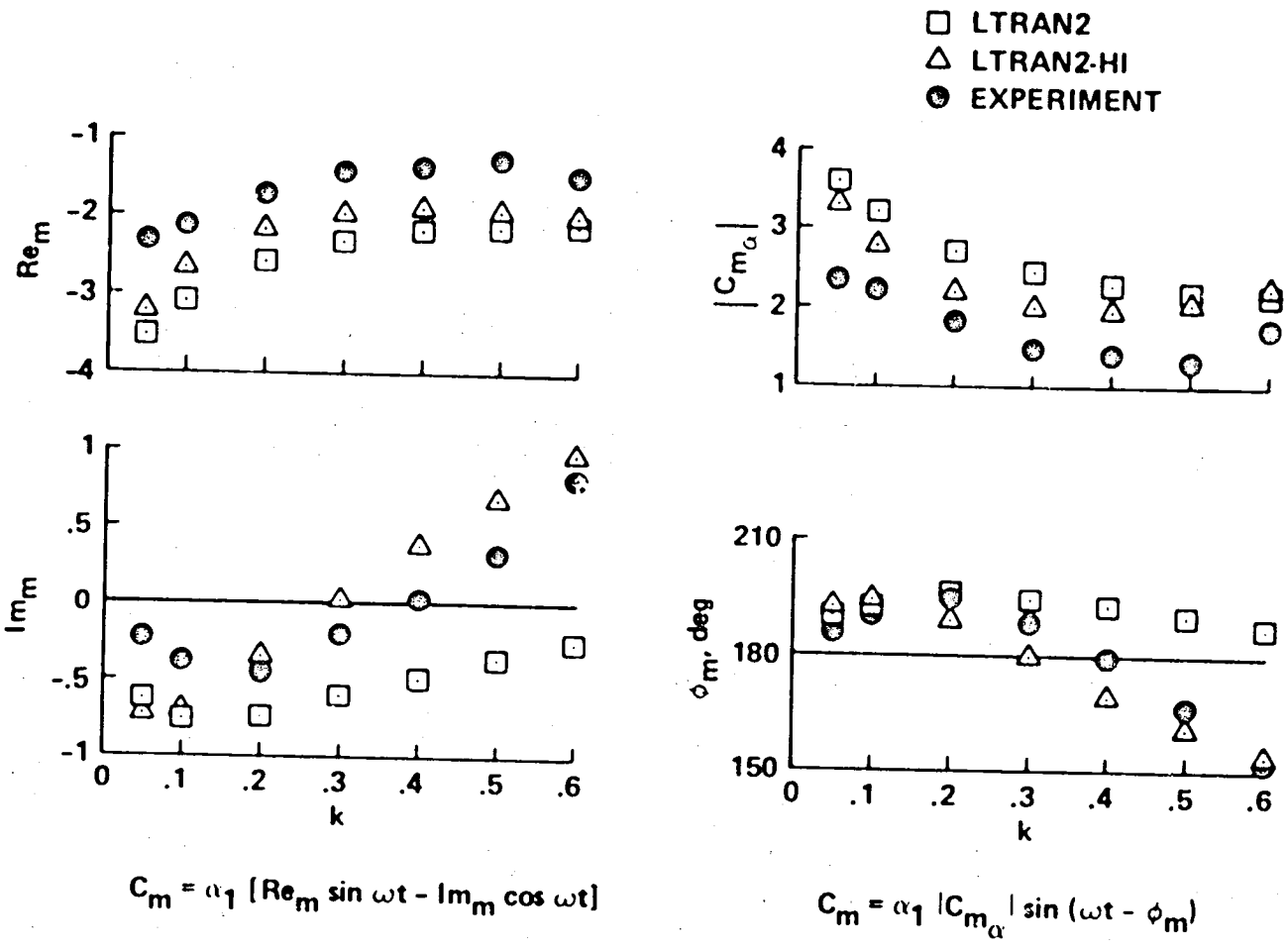

(a) Real and imaginary components.

(b) Amplitude and phase.

Figure 5.- Leading-edge moment coefficients vs reduced frequency for a pitching NACA 64A010 airfoil, $M_\infty = 0.8$, $k = \omega c/U_\infty$, $\alpha = \alpha_0 + \alpha_1 \sin \omega t$.

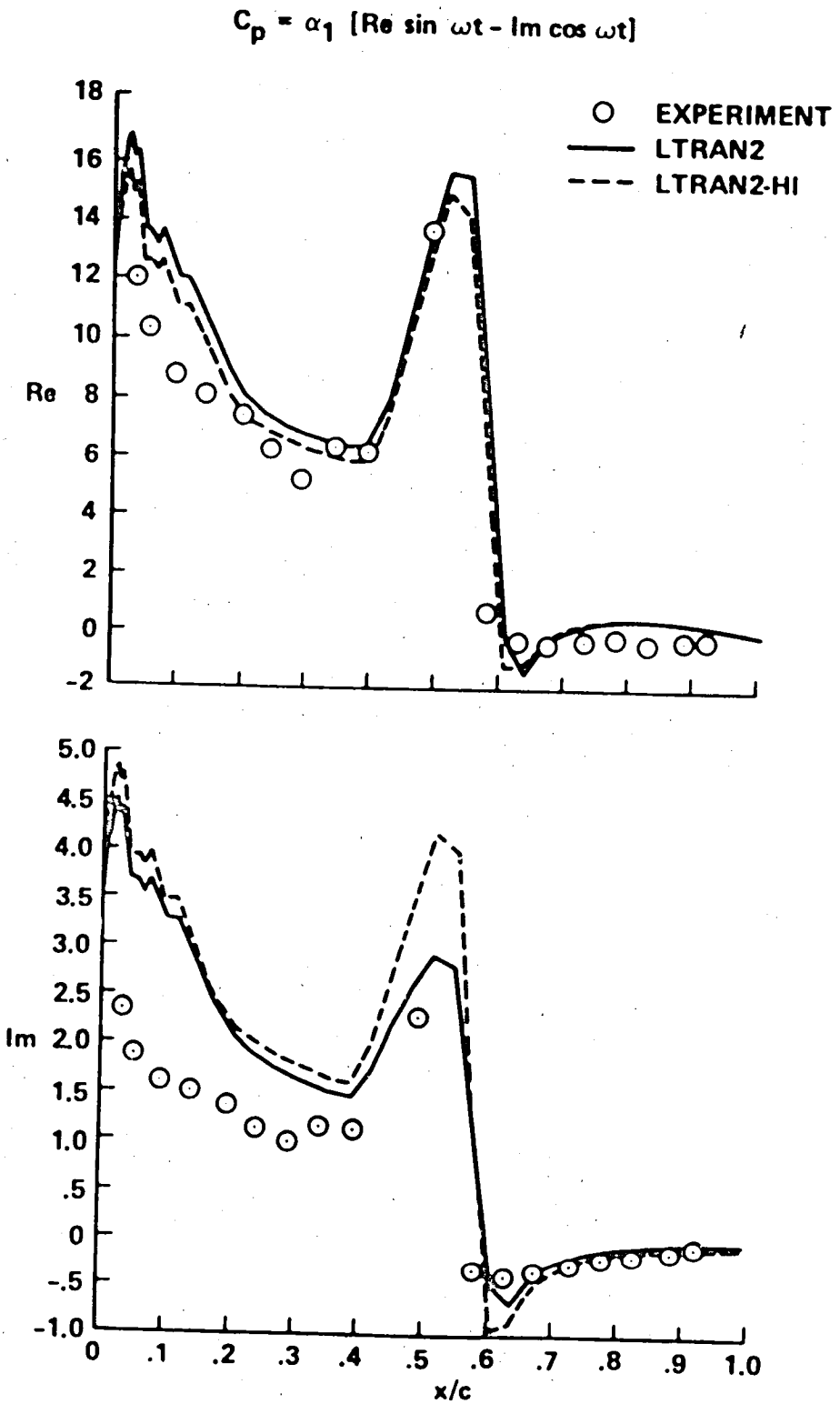

Figure 6.- Unsteady lower-surface pressure coefficients (real and imaginary components) for a pitching NACA 64A010 airfoil, $M_\infty = 0.8$, $k \equiv \omega c/U_\infty = 0.05$.

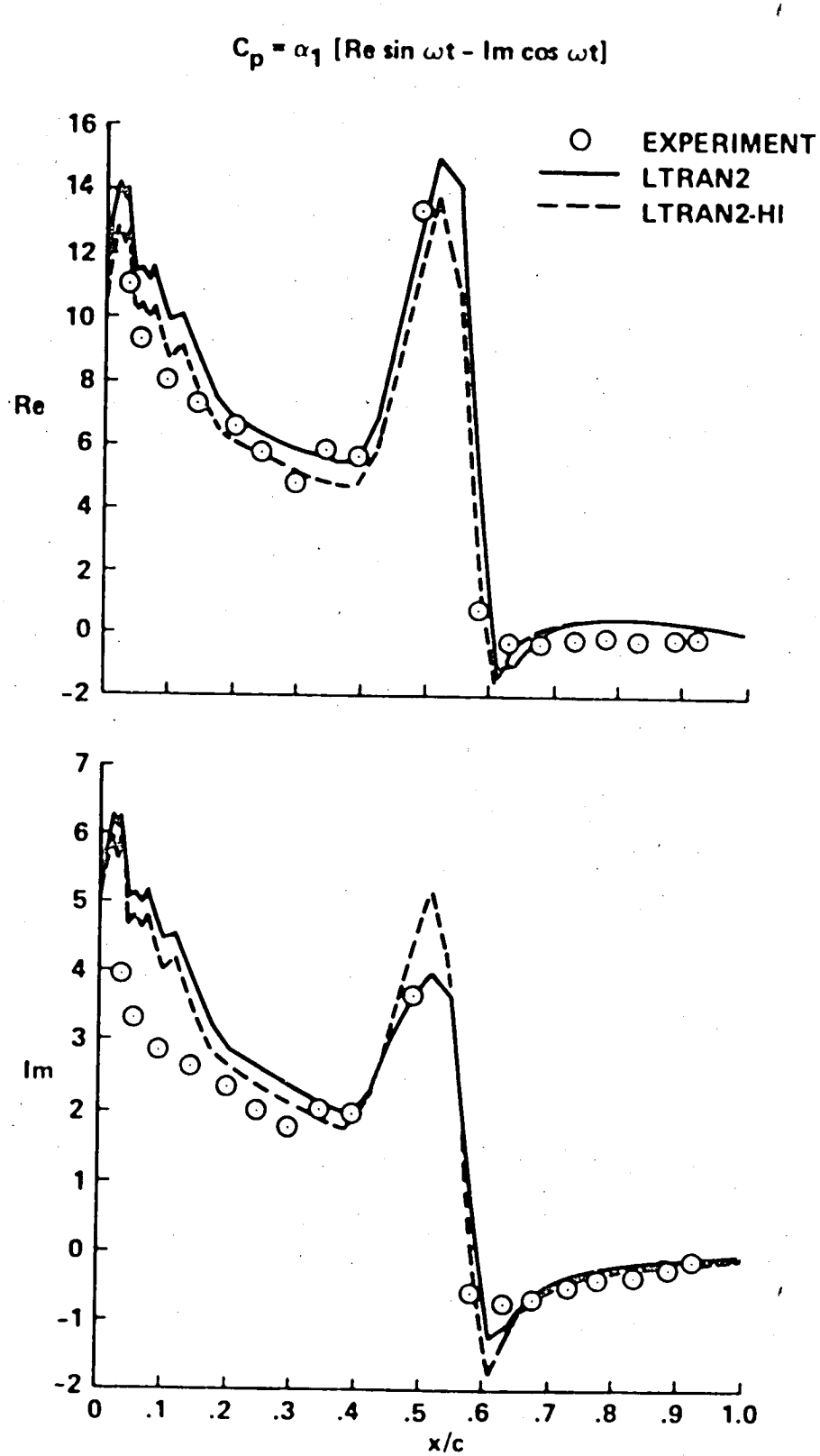

(a) Real and imaginary components.

Figure 7.- Unsteady lower-surface pressure coefficients for a pitching NACA 64A010 airfoil, $M_\infty = 0.8$, $k \equiv \omega c/U_\infty = 0.1$.

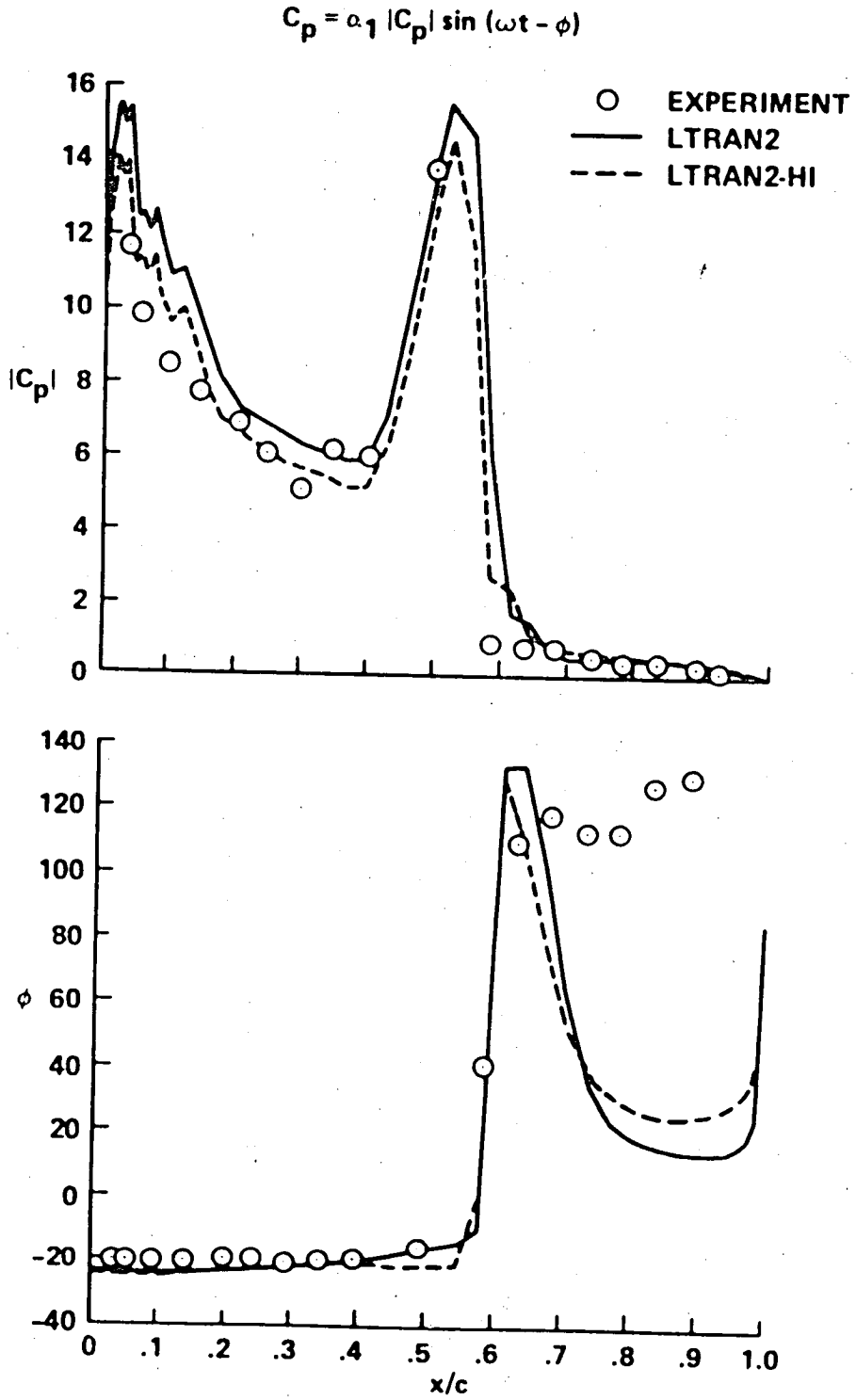

(b) Amplitude and phase.

Figure 7.- Concluded.

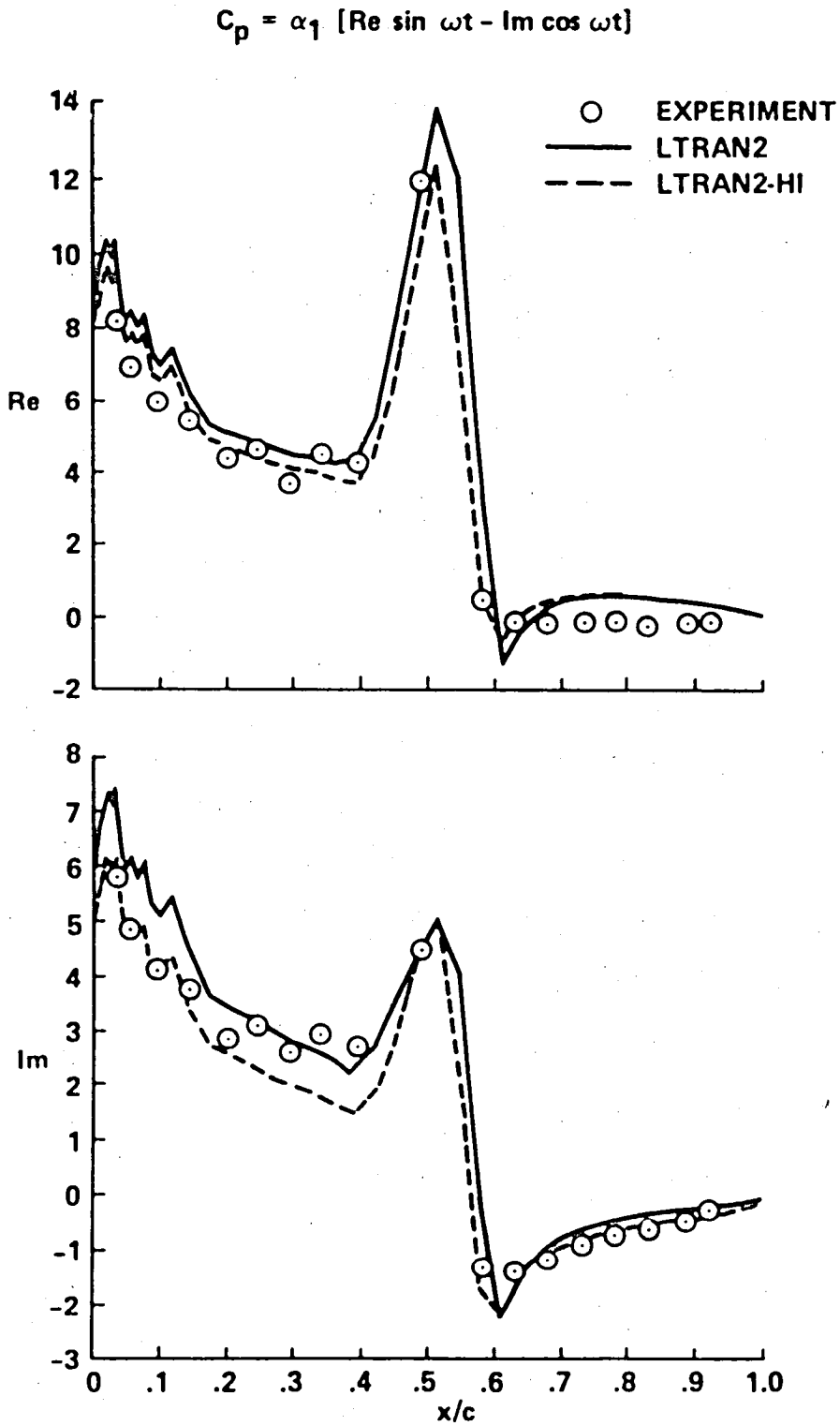

Figure 8.- Unsteady lower-surface pressure coefficients (real and imaginary components) for a pitching NACA 64A010 airfoil, $M_\infty = 0.8$, $k \equiv \omega c/U_\infty = 0.2$.

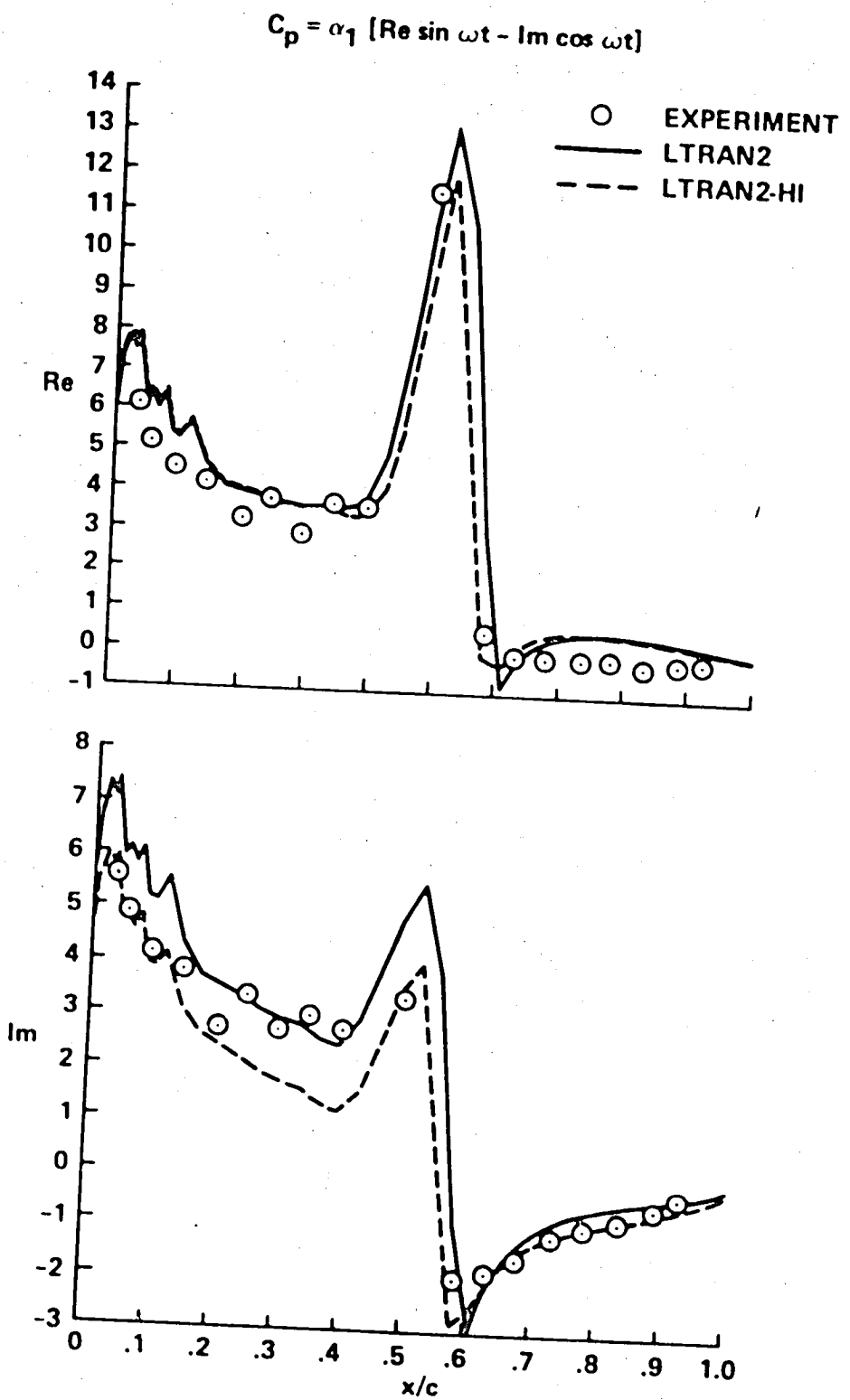

Figure 9.- Unsteady lower-surface pressure coefficients (real and imaginary components) for a pitching NACA 64A010 airfoil, $M_\infty = 0.8$, $k = \omega c/U_\infty = 0.3$.

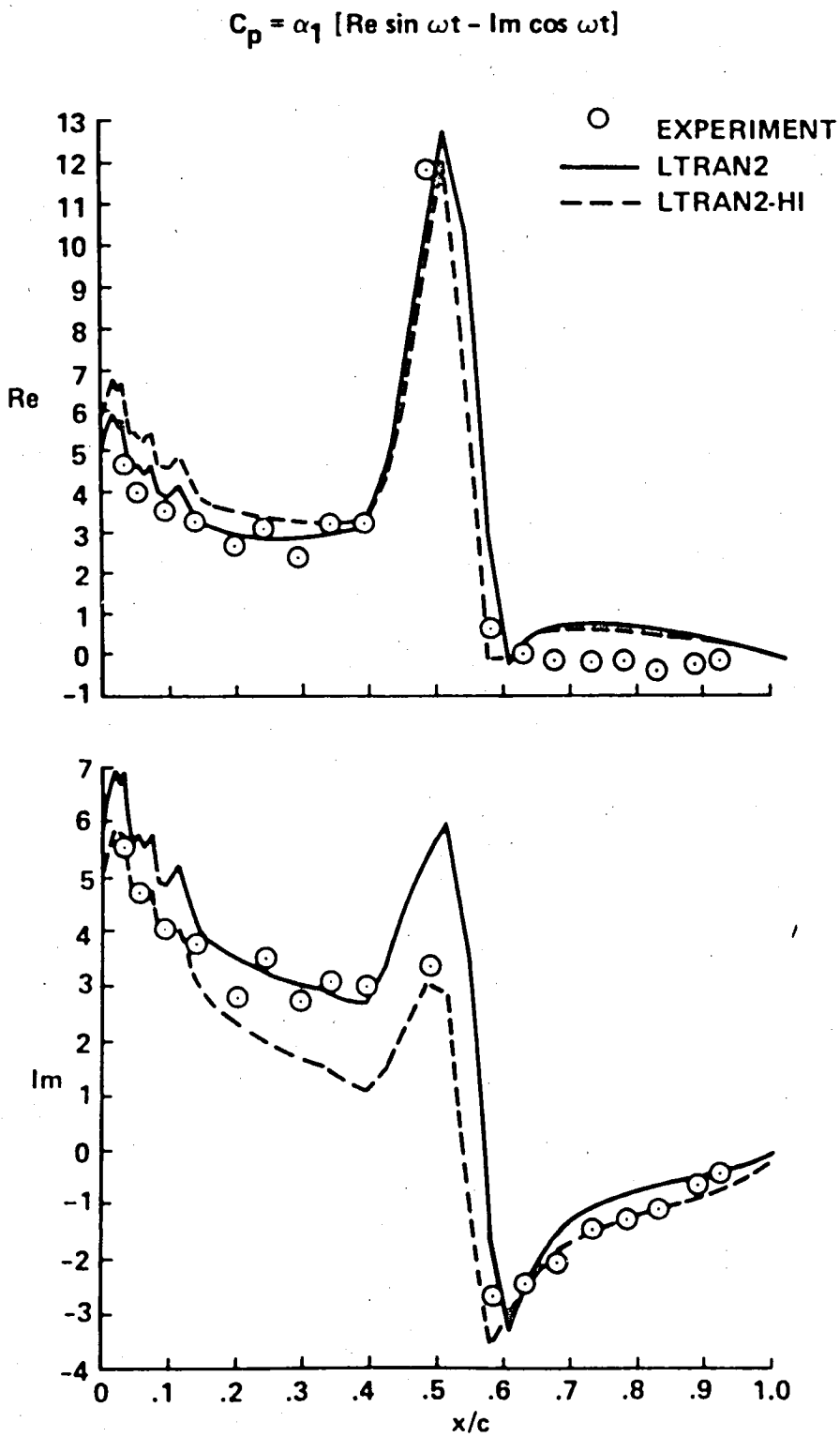

Figure 10.- Unsteady lower-surface pressure coefficients (real and imaginary components) for a pitching NACA 64A010 airfoil, $M_\infty = 0.8$, $k \equiv \omega c/U_\infty = 0.4$.

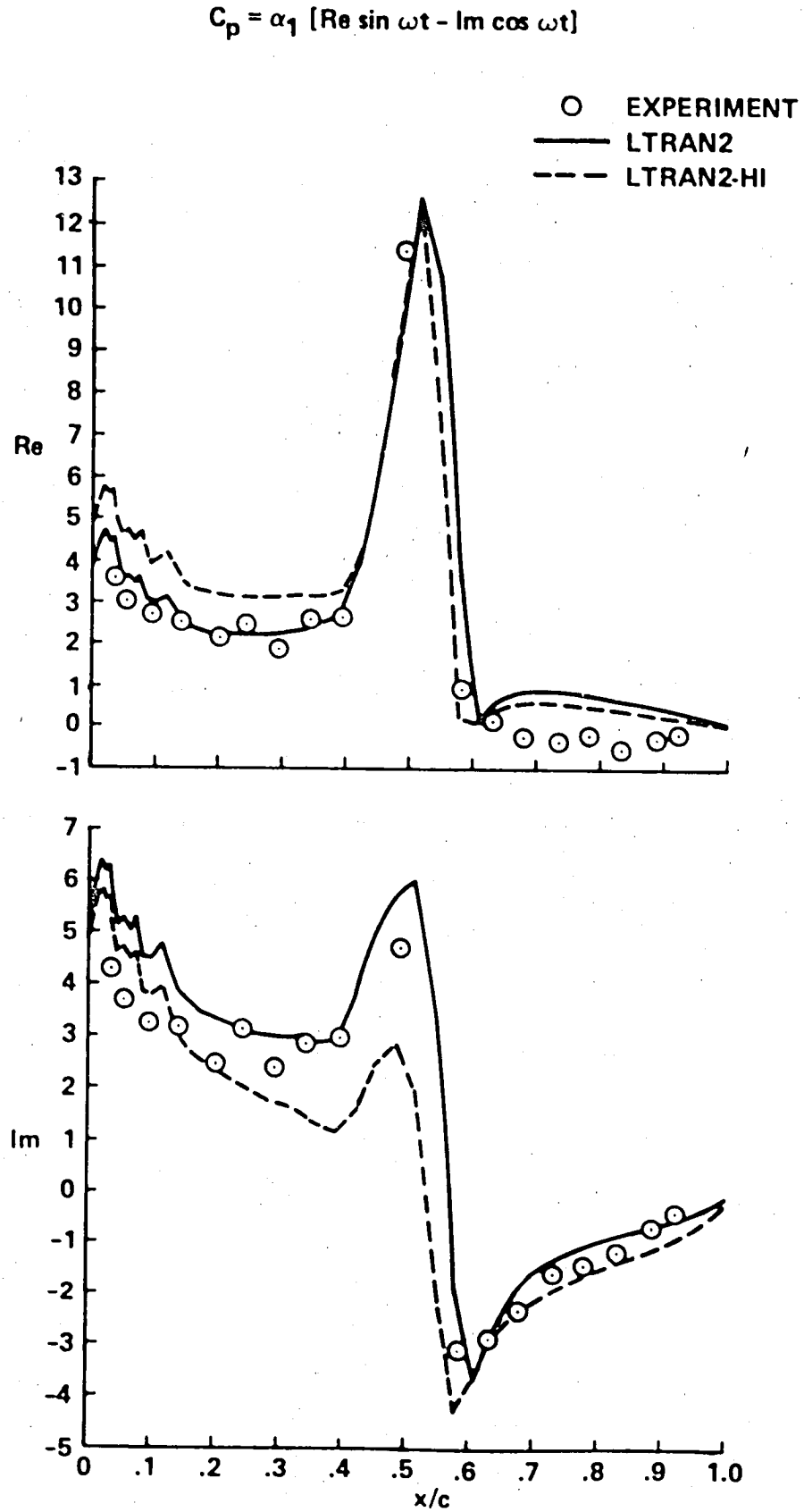

Figure 11.- Unsteady lower-surface pressure coefficients (real and imaginary components) for a pitching NACA 64A010 airfoil, $M_\infty = 0.8$, $k \equiv \omega c/U_\infty = 0.5$.

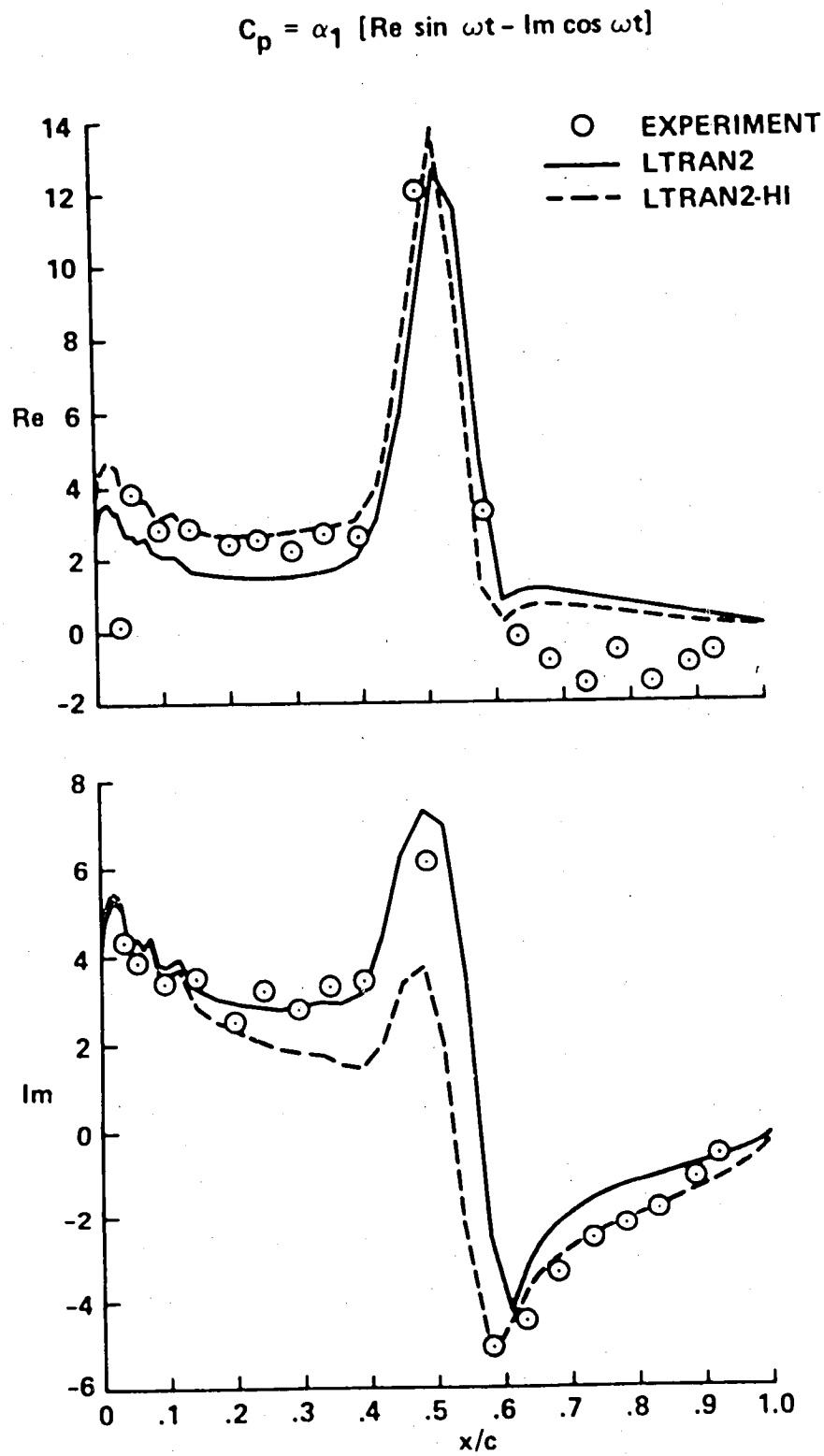

Figure 12.- Unsteady lower-surface pressure coefficients (real and imaginary components) for a pitching NACA 64A010 airfoil, $M_\infty = 0.8$, $k \equiv \omega c/U_\infty = 0.6$.